



Contents lists available at ScienceDirect

Inorganica Chimica Acta

journal homepage: [www.elsevier.com/locate/ica](http://www.elsevier.com/locate/ica)

Research paper

## Cu(II) complexes with hydrazone-functionalized phenanthrolines as self-activating metallonucleases

Julian Heinrich, Jessica Stubbe, Nora Kulak\*

Institut für Chemie und Biochemie, Freie Universität Berlin, Fabeckstraße 34/36, 14195 Berlin, Germany

## ARTICLE INFO

## Article history:

Received 24 July 2017

Received in revised form 5 November 2017

Accepted 8 November 2017

Available online xxx

## Keywords:

Copper(II) complexes

Self-activating metallonucleases

Phenanthroline

Hydrazone

DNA cleavage

DNA binding

## ABSTRACT

Cu(II) phenanthroline complexes are able to cleave DNA and show cytotoxic activity against cancer cells. Also, the biological activity of hydrazone-based compounds has been reported in the literature. This motivated us to combine these two systems. Hydrazone-functionalized phenanthroline ligands with acetyl and benzoyl substituents were synthesized and characterized. The DNA cleavage activity of the corresponding Cu(II) complexes **3** and **4** was compared to the one of the well-known  $[\text{Cu}(\text{phen})_2]^{2+}$  complex (**1**) and  $[\text{Cu}(\text{phenD})_2]^{2+}$  complex (**2**, phenD = 1,10-phenanthroline-5,6-dione, the precursor of hydrazone-functionalized phenanthrolines). In the presence of ascorbate, but also in its absence, oxidative cleavage of DNA was proven by quenching therein involved reactive oxygen species (ROS), specifically hydrogen peroxide and superoxide anion radicals. Only complexes **2–4** were active in the absence of ascorbate, but not  $[\text{Cu}(\text{phen})_2]^{2+}$  (**1**). The surprising occurrence of ROS in the absence of any activating agent indicates that **2–4** represent self-activating artificial metallonucleases. Thereby, self-activation was most prominent for the novel hydrazone-based complexes **3** and **4**. Cyclic voltammetry and circular dichroism spectroscopy were applied to get an insight in redox behavior and DNA binding characteristics of the Cu(II) complexes and thus to explain their different nuclease activity.

© 2017 Elsevier B.V. All rights reserved.

## 1. Introduction

In the last few decades 1,10-phenanthroline (phen) has played an important role in coordination chemistry due to its broad field of applications. This ligand has received enormous interest due to its rich functionalization chemistry, its chelating properties towards several metal ions and biological activity of the corresponding metal complexes [1]. The derivatization of phenanthroline in positions 2 and 9 as well as 5 to hydrazones is well investigated. Thereby hydrazone-functionalized phenanthrolines can coordinate several metal ions, e.g. Re(I), Pb(IV), Sn(IV), Gd(III), La(III) and Cu(II) at either the phenanthroline moiety or both the phenanthroline and hydrazone moieties [2–5]. To the best of our knowledge, coordination of phenanthrolines with hydrazone functionalization in position 5 to Cu(II) ions over the phenanthroline scaffold has not been described before.

The Cu(II) complex of the unsubstituted phenanthroline,  $[\text{Cu}(\text{phen})_2]^{2+}$ , is still up to date one of the most efficient artificial metallonucleases since its discovery in the '70s [6–8]. On the other hand, hydrazone-based compounds have been exploited for their

versatile biological activity [9]. Combining both systems to form a Cu(II) complex with hydrazone-functionalized phenanthrolines could lead to novel artificial nucleases with enhanced biological activity. Such an approach is of general interest in biological/medicinal inorganic chemistry, but it also bears potential for the development of well-tolerated anticancer drugs. The most successful metal-based anticancer drug, cisplatin, suffers from causing severe side effects. Whereas a compound comprising copper as an endogenous metal, instead of platinum, could guarantee lower systemic toxicity [10].

In general there are two common pathways, in which artificial Cu(II) metallonucleases degrade DNA: oxidative and hydrolytic cleavage. The latter cleavage mechanism involves the phosphate backbone of DNA, and is enzymatically reversible [11]. The oxidative cleavage mechanism implies a double-strand break subsequent to the generation of reactive oxygen species (ROS) [12,13]. The latter cleaving mechanism is irreversible, which is important for the potential application of such metallonucleases as chemotherapeutic agents. In general, the oxidative DNA cleavage is common for complexes, which can be activated by a reductant. They can then initiate the generation of ROS in an aerobic environment while being re-oxidized themselves [14,15]. Besides the initiation of redox processes, another possibility for the activation

\* Corresponding author.

E-mail address: [nora.kulak@fu-berlin.de](mailto:nora.kulak@fu-berlin.de) (N. Kulak).

of metallonucleases is using light as a trigger. This has been broadly covered in the literature [16]. Some of the rarest DNA cleaving agents are the self-activating metallonucleases. In this case, the ligand should be redox active replacing the external reducing agent. On the one hand for Cu(II) complexes, the ligand could be oxidized – as seen with prodigiosins or hydrazones – to create a reduced Cu(I) species, which in turn generates ROS in a cascade manner as described above [17–19]. On the other hand, the reduced form of the ligand can be stabilized – as seen with hydroxy-salens – to gain a rare Cu(III) species, which can bind molecular oxygen for the generation of superoxide anion radicals without the need for any reducing agent [20].

Only a few examples of self-activating metallonucleases based on Cu(II) complexes with either phenanthroline or hydrazone ligands, where DNA is cleaved by generation of ROS in the absence of a reducing agent, are described in literature [20–22]. Thus, the aim of this work was the synthesis of novel Cu(II) complexes with hydrazone-functionalized phenanthrolines and the evaluation of their biological activity regarding the DNA cleavage properties in a self-activating manner.

## 2. Experimental part

### 2.1. Materials and methods

All chemicals and solvents were purchased from Acros Organics, Alfa Aesar, Fisher Scientific, Carl Roth or Sigma Aldrich and were used without further purification. <sup>1</sup>H NMR spectra of the ligands were recorded in CDCl<sub>3</sub> or DMSO *d*<sub>6</sub> on a Jeol ECX 400 spectrometer at room temperature. Chemical shifts are given relative to TMS with positive  $\delta$  values indicating a low field shift. The characterization of the ligands and their Cu(II) complexes was performed via elemental analysis on a vario EL CHNS, UV/Vis spectroscopy on an Agilent Cary 100 instrument and electrospray ionization mass spectrometry (ESI-MS) on an Agilent 6210 ESI-TOF using methanol and ethanol, respectively, for the ligands and acetonitrile for the complexes (flow rate 10  $\mu$ L/min).

### 2.2. Synthesis of the ligands

#### 2.2.1. 1,10-Phenanthroline-5,6-dione (phenD)

The ligand phenD was prepared by oxidation of commercially available phen according to the literature [23].

A mixture of potassium bromide (29.750 g, 0.250 mol) and phen (5.000 g, 0.028 mol) in 96% sulfuric acid (75 mL) and 65% nitric acid (37.5 mL) was refluxed and stirred for 2 h. The reaction mixture was diluted with water (1000 mL) and neutralized with sodium bicarbonate. The mixture was then extracted three times with dichloromethane (3  $\times$  300 mL). The organic phase was dried over sodium sulfate for 30 min and the solvent was evaporated under reduced pressure. The obtained crude product was recrystallized in methanol to obtain phenD as a yellow powder. Yield: 30%. *Anal.* Elemental analysis: Calc.: C<sub>12</sub>H<sub>6</sub>N<sub>2</sub>O<sub>2</sub>·0.2 CH<sub>3</sub>OH (%): C, 67.65; H, 3.16; N, 12.93. Found: C, 67.28; H, 2.95; N, 13.23. <sup>1</sup>H NMR (400 MHz, CDCl<sub>3</sub>):  $\delta$  = 7.59 (dd, 2H<sup>phen</sup>, *J* = 4.68 Hz, *J* = 7.87 Hz); 8.50 (dd, 2H<sup>phen</sup>, *J* = 1.85 Hz, *J* = 7.87 Hz); 9.12 (dd, 2H<sup>phen</sup>, *J* = 1.84 Hz, *J* = 4.70 Hz) ppm. HR ESI-MS: *m/z* [M + H]<sup>+</sup> Calc.: 211.0502, Found: 211.0533; [M + Na]<sup>+</sup> Calc.: 233.0321, Found: 233.0365.

#### 2.2.2. Hydrazone-functionalized phenanthrolines

The ligands *N'*-(6-oxo-1,10-phenanthroline-5(6H)-ylidene)acetohydrazide (phenAH) and -benzohydrazide (phenBH) were prepared according to the following general procedure by condensing phenD with the appropriate hydrazide [2].

The respective hydrazide was dissolved in ethanol, phenD and a catalytic amount of *p*-toluenesulfonyl chloride was added dropwise. The mixture was stirred under reflux for 6 h. After storing overnight at –24 °C the formed precipitate was filtered off. The crude product was recrystallized in ethanol to obtain the respective hydrazone-functionalized phenanthroline.

2.2.2.1. *N'*-(6-oxo-1,10-phenanthroline-5(6H)-ylidene)acetohydrazide (phenAH). Acetohydrazide (0.194 g, 2.515 mmol), ethanol (100 mL), phenD (0.505 g, 2.403 mmol) and *p*-toluenesulfonyl chloride (0.015 g, 0.077 mmol) were used for the synthesis of the ligand phenAH, a yellow solid. Yield: 51%. *Anal.* Elemental analysis: Calc.: C<sub>14</sub>H<sub>10</sub>N<sub>4</sub>O<sub>2</sub> (%): C, 63.15; H, 3.79; N, 21.04. Found: C, 63.15; H, 3.95; N, 21.03. <sup>1</sup>H NMR (400 MHz, DMSO *d*<sub>6</sub>):  $\delta$  = 2.49 (s, 3H<sup>acetyl</sup>); 7.73 (m, 2H<sup>phen</sup>); 8.59 (m, 2H<sup>phen</sup>); 8.87–9.11 (dd, 2H<sup>phen</sup>, *J* = 4.40 Hz, *J* = 90.06 Hz); 13.96 (s, 1H<sup>H</sup>) ppm. HR ESI-MS: *m/z* [M + H]<sup>+</sup> Calc.: 267.0877, Found: 267.0892; [M + Na]<sup>+</sup> Calc.: 289.0696, Found: 289.0741.

2.2.2.2. *N'*-(6-oxo-1,10-phenanthroline-5(6H)-ylidene)benzohydrazide (phenBH). Benzhydrazide (0.324 g, 2.380 mmol), ethanol (100 mL), phenD (0.502 g, 2.390 mmol) and *p*-toluenesulfonyl chloride (0.013 g, 0.070 mmol) were utilized for the synthesis of the ligand phenBH, a yellow-orange solid. Yield: 78% (literature: 83% [2]). *Anal.* Elemental analysis: Calc.: C<sub>19</sub>H<sub>12</sub>N<sub>4</sub>O<sub>2</sub> (%): C, 69.51; H, 3.68; N, 17.06. Found: C, 69.59; H, 3.76; N, 17.12. <sup>1</sup>H NMR (400 MHz, DMSO *d*<sub>6</sub>):  $\delta$  = 7.70 (m, 5H<sup>benzoyl</sup>); 8.01 (d, 2H<sup>phen</sup>, *J* = 7.87 Hz); 8.64 (dd, 2H<sup>phen</sup>, *J* = 8.03 Hz, *J* = 16.99 Hz); 8.90–9.11 (dd, 2H<sup>phen</sup>, *J* = 2.77 Hz, *J* = 86.39 Hz) ppm. HR ESI-MS: *m/z* [M + H]<sup>+</sup> Calc.: 329.1033, Found: 329.1060; [M + Na]<sup>+</sup> Calc.: 351.0852, Found: 351.0893.

### 2.3. Synthesis of the Cu(II) complexes

The Cu(II) complexes were prepared according to the following general procedure based on literature reports for the synthesis of the compounds [Cu(phen)<sub>2</sub>](NO<sub>3</sub>)<sub>2</sub> (**1**(NO<sub>3</sub>)<sub>2</sub>) and [Cu(phenD)<sub>2</sub>](NO<sub>3</sub>)<sub>2</sub> (**2**(NO<sub>3</sub>)<sub>2</sub>) [24,25].

Cu(NO<sub>3</sub>)<sub>2</sub>·3H<sub>2</sub>O was dissolved in a small amount of ethanol. The ligand was suspended in ethanol and the suspension was heated up to 60 °C before the Cu(NO<sub>3</sub>)<sub>2</sub>·3H<sub>2</sub>O solution was slowly added. A 1:2 ratio of Cu(II):ligand was ensured, when both components were combined. The occurring blue (**1**), green (**2**), red-brownish (**3**) or green-brownish (**4**) solution was heated to reflux for 1 h. Upon storage of the solution at –24 °C overnight the turquoise **1** (NO<sub>3</sub>)<sub>2</sub>, mint green **2**(NO<sub>3</sub>)<sub>2</sub>, brown **3**(NO<sub>3</sub>)<sub>2</sub> and lime green **4** (NO<sub>3</sub>)<sub>2</sub> precipitates were filtered off and dried *in vacuo*.

#### 2.3.1. [Cu(phen)<sub>2</sub>](NO<sub>3</sub>)<sub>2</sub> (**1**(NO<sub>3</sub>)<sub>2</sub>)

Cu(NO<sub>3</sub>)<sub>2</sub>·3H<sub>2</sub>O (0.135 g, 0.560 mmol), phen (0.200 g, 0.110 mmol) and 30 mL ethanol were used for the synthesis of **1**(NO<sub>3</sub>)<sub>2</sub>, a turquoise solid. Yield: 73%. *Anal.* Elemental analysis: Calc.: C<sub>24</sub>H<sub>16</sub>CuN<sub>6</sub>O<sub>6</sub> (%): C, 52.61; H, 2.94; N, 15.34. Found: C, 52.63; H, 3.06; N, 15.41. HR ESI-MS: *m/z* [**1**]<sup>2+</sup> Calc.: 211.5330, Found: 211.5376; [**1** + NO<sub>3</sub>]<sup>+</sup> Calc.: 485.0544, Found: 485.0612; [**1** + Cl]<sup>+</sup> Calc.: 458.0354, Found: 458.0424.

#### 2.3.2. [Cu(phenD)<sub>2</sub>](NO<sub>3</sub>)<sub>2</sub> (**2**(NO<sub>3</sub>)<sub>2</sub>)

Cu(NO<sub>3</sub>)<sub>2</sub>·3H<sub>2</sub>O (0.059 g, 0.244 mmol), phenD (0.103 g, 0.488 mmol) and 15 mL ethanol were used for the synthesis of **2**(NO<sub>3</sub>)<sub>2</sub>, a mint green solid. Yield: 71%. *Anal.* Elemental analysis: Calc.: C<sub>24</sub>H<sub>12</sub>CuN<sub>6</sub>O<sub>10</sub> (%): C, 47.42; H, 1.99; N, 13.82. Found: C, 47.58; H, 2.04; N, 13.91. HR ESI-MS: *m/z* [**2**]<sup>2+</sup> Calc.: 241.5072, Found: 241.5118; [**2** + NO<sub>3</sub>]<sup>+</sup> Calc.: 545.0027, Found: 545.0122; [**2** + Cl]<sup>+</sup> Calc.: 517.9838, Found: 517.9951.

### 2.3.3. $[\text{Cu}(\text{phenAH})_2](\text{NO}_3)_2 \cdot 3(\text{NO}_3)_2$

$\text{Cu}(\text{NO}_3)_2 \cdot 3\text{H}_2\text{O}$  (0.068 g, 0.282 mmol), phenAH (0.150 g, 0.563 mmol) and 20 mL ethanol were used for the synthesis of **3**( $\text{NO}_3$ )<sub>2</sub>, a brown solid. Yield: 15%. Anal. Elemental analysis: Calc.: C<sub>28</sub>H<sub>20</sub>-CuN<sub>10</sub>O<sub>10</sub>·2.5 H<sub>2</sub>O·0.5 C<sub>2</sub>H<sub>5</sub>OH (%): C, 44.19; H, 3.58; N, 17.77. Found: C, 43.69; H, 3.07; N, 17.29. Note: Although the agreement of calculated and found values is slightly outside the commonly accepted range of 0.4%, we observed the same DNA cleavage activity for this complex as for the *in situ* prepared compound (*vide infra*). HR ESI-MS: *m/z* [**3**]<sup>2+</sup> Calc.: 297.5446, Found: 297.5493; [**3** + NO<sub>3</sub>]<sup>+</sup> Calc.: 657.0776, Found: 657.0872; [**3** + Cl]<sup>+</sup> Calc.: 630.0587, Found: 630.0672.

### 2.3.4. $[\text{Cu}(\text{phenBH})_2](\text{NO}_3)_2 \cdot 4(\text{NO}_3)_2$

$\text{Cu}(\text{NO}_3)_2 \cdot 3\text{H}_2\text{O}$  (0.055 g, 0.228 mmol), phenBH (0.150 g, 0.457 mmol) and 20 mL ethanol were used for the synthesis of **4**( $\text{NO}_3$ )<sub>2</sub>, a lime green solid. Yield: 50%. Anal. Elemental analysis: Calc.: C<sub>38</sub>H<sub>24</sub>CuN<sub>10</sub>O<sub>10</sub> (%): C, 54.06; H, 2.87; N, 16.59. Found: C, 54.04; H, 3.17; N, 16.57. HR ESI-MS: *m/z* [**4**]<sup>2+</sup> Calc.: 359.5603, Found: 359.5660; [**4** + NO<sub>3</sub>]<sup>+</sup> Calc.: 781.1089, Found: 781.1212; [**4** + Cl]<sup>+</sup> Calc.: 754.0900, Found: 754.1039.

## 2.4. Cyclic voltammetry

Cyclic voltammograms were recorded with a PAR VersaStat 4 potentiostat (Ametek) by working in anhydrous and degassed dimethylformamide with 0.1 M NBu<sub>4</sub>PF<sub>6</sub> (dried, >99.0%, electrochemical grade, Fluka) as supporting electrolyte. Concentrations of the Cu(II) complexes (**1–4**) were about 10<sup>-4</sup> M. A three-electrode setup was used with a glassy carbon working electrode, a coiled platinum wire as counter electrode, and a coiled silver wire as a pseudoreference electrode. The ferrocene/ferrocenium redox couple was used as internal reference.

## 2.5. DNA cleavage studies

Plasmid DNA pBR322 was purchased from Carl Roth. All DNA cleavage experiments were performed at least in triplicate in order to ensure reproducibility.

Metal complex solutions (**1–4**) were prepared *in situ* as follows: 500 μL of a 0.84 mM ligand solution in DMSO and 500 μL of an aqueous 0.40 mM CuCl<sub>2</sub> solution were combined resulting in 1 mL of a 0.40 mM complex solution in water:DMSO 1:1 (Cu:ligand ratio 1:2.1).

### 2.5.1. General procedure

For the investigation of oxidative DNA cleavage activity of the complexes a mixture of plasmid DNA pBR322 (0.025 μg/μL) buffered in MOPS (50 mM, pH 7.4) was incubated for 2 h at 37 °C with the respective compound (25 μM CuCl<sub>2</sub>/52.5 μM ligand from the above described solutions) in the presence of ascorbate (1 mM) as reducing agent or in its absence. For the latter case double concentrations of the complexes were used (50 μM CuCl<sub>2</sub>/105 μM ligand). Thereby all samples contained 12.5% DMSO. Gel electrophoresis was carried out for 2 h at 40 V using a 1% agarose gel containing ethidium bromide (0.2 μg/mL) in 0.5X TBE buffer. The bands of supercoiled (S), open-circular/nicked (N), and linear (L) DNA were visualized by fluorescence imaging of intercalating ethidium bromide on a Bio-Rad GelDoc EZ Imager. Data analysis was performed with Bio-Rad's Image Lab Software (Version 3.0). Due to the decreased affinity of ethidium bromide to supercoiled DNA a correction factor of 1.22 was used [26].

### 2.5.2. Reactive oxygen species (ROS)

For the determination of ROS exemplarily generated by complex **3** (12.5 μM CuCl<sub>2</sub>/26.25 μM ligand) the general DNA cleaving

procedure as described above was applied in the presence of ascorbate (1 mM) and one of the following ROS scavengers: DMSO (400 mM), NaN<sub>3</sub> (10 mM), pyruvate (2.5 mM) and superoxide dismutase (SOD, 625 U/mL). In the case of pyruvate as a ROS scavenger a MOPS buffer concentration of 100 mM was needed to keep the pH value constant at 7.4. Combining the ROS scavenger pyruvate (hydrogen peroxide scavenger) with SOD ensured immediate degradation of enzymatically produced hydrogen peroxide. Additionally, one sample included all scavengers described above.

Furthermore, to investigate the self-activating DNA cleavage of complex **3** (37.5 μM CuCl<sub>2</sub>/78.5 μM ligand) the same experiment described above was carried out with all ROS scavengers in the absence of ascorbate as reducing agent.

### 2.5.3. Bis-nitrophenyl phosphate (BNPP) assay

For the investigation of hydrolytic DNA cleavage activity a mixture of BNPP (50 μM) buffered in MOPS buffer (50 mM, pH 7.4) was incubated exemplarily with complex **3** (50 μM CuCl<sub>2</sub>/105 μM ligand or 100 μM CuCl<sub>2</sub>/210 μM ligand) for 2 h at 37 °C. As a positive control the enzymatic BNPP cleavage by phosphodiesterase I (0.05 U/mL) was carried out. The volume of all samples was adjusted to 1 mL, all samples contained 12.5% DMSO. Following the incubation, the degree of BNPP cleavage was monitored UV/Vis spectroscopically in the range of 200–550 nm for each sample with the respective baseline (the baseline included all compounds except BNPP).

## 2.6. Circular dichroism (CD) spectroscopy

CD spectra of calf thymus (CT) DNA (100 μM) in MOPS buffer (50 mM, pH 7.4) were recorded on a Jasco J-810 spectrometer in a range of 220–320 nm with a measuring velocity of 100 nm/min and a data point interval of 0.1 nm. Cu(II) complexes **1–4** were added stepwise (5 μM CuCl<sub>2</sub>/10.5 μM ligand to 15 μM CuCl<sub>2</sub>/31.5 μM ligand) to investigate their mode of interaction towards DNA. The volume of all samples was adjusted to 1 mL, all samples contained 10% DMSO.

## 3. Results and discussion

### 3.1. Synthesis of the Cu(II) complexes

Proceeding from the commercially available 1,10-phenanthroline (phen) the oxidized compound 1,10-phenanthroline-5,6-dione (phenD) was synthesized according to the literature [23]. *N'*-(6-Oxo-1,10-phenanthroline-5(6*H*)-ylidene)benzohydrazide (phenBH) was prepared by condensing phenD with benzohydrazide [2]. This synthetic route for hydrazone-functionalization in position 5 of phenanthrolines was adjusted to prepare the compound *N'*-(6-oxo-1,10-phenanthroline-5(6*H*)-ylidene)acetohydrazide (phenAH), which has not been described in the literature before. All ligands (phenD, phenBH, phenAH) were characterized *via* elemental analysis, <sup>1</sup>H NMR spectroscopy and high-resolution mass spectrometry (Section 2.2.).

The synthesis of the novel Cu(II) complexes of phenBH and phenAH was based on a procedure for the synthesis of Cu(II) complexes of phen and phenD [24,25]. All Cu(II) complexes [Cu(phen)<sub>2</sub>](NO<sub>3</sub>)<sub>2</sub> (**1**(NO<sub>3</sub>)<sub>2</sub>), [Cu(phenD)<sub>2</sub>](NO<sub>3</sub>)<sub>2</sub> (**2**(NO<sub>3</sub>)<sub>2</sub>), [Cu(phenAH)<sub>2</sub>](NO<sub>3</sub>)<sub>2</sub> (**3**(NO<sub>3</sub>)<sub>2</sub>) and [Cu(phenBH)<sub>2</sub>](NO<sub>3</sub>)<sub>2</sub> (**4**(NO<sub>3</sub>)<sub>2</sub>) were characterized *via* elemental analysis and high resolution mass spectrometry (Section 2.3.) as well as UV/Vis spectroscopy.

UV/Vis spectra of the isolated complexes (NO<sub>3</sub><sup>-</sup> counter ions) as well as the *in situ* prepared complexes (Cl<sup>-</sup> counterions) **1–4** revealed that in aqueous solution presumably the same species were present during DNA cleavage for these complexes prepared

by different means (cf. S11). Whereas **1** and **2** show characteristic d-d transition bands at  $\sim 700$  nm (see inset in S11) [25], **3** and **4** exhibit broad, intense MLCT bands (400–600 nm) instead. The latter indicates formation of Cu(I) species in aqueous solution [25] (*vide infra*).

The composition and structures of the complexes are shown in Chart 1. To the best of our knowledge, **3** and **4** represent the first Cu(II) complexes of phenanthroline with hydrazone-functionalization in position 5.

### 3.2. DNA cleavage studies

#### 3.2.1. Nuclease activity

In order to investigate the oxidative DNA cleavage activity of  $[\text{Cu}(\text{phen})_2]^{2+}$  (**1**),  $[\text{Cu}(\text{phenD})_2]^{2+}$  (**2**),  $[\text{Cu}(\text{phenAH})_2]^{2+}$  (**3**) and  $[\text{Cu}(\text{phenBH})_2]^{2+}$  (**4**), their ability to convert supercoiled (S) plasmid DNA into open-circular/nicked (N) and linear (L) DNA forms was monitored by agarose gel electrophoresis. Plasmid DNA pBR322 was incubated either with the complexes at  $25 \mu\text{M}$  concentration in the presence of the reducing agent ascorbate (1 mM) or with the respective complexes at  $50 \mu\text{M}$  concentration in the absence of ascorbate for 2 h at  $37^\circ\text{C}$ . The pH value was kept constant at 7.4 using MOPS buffer (50 mM). We have chosen this buffer instead of the more frequently used Tris buffer in order to avoid potential competitive coordination of the buffer molecules to Cu(II) [27]. Furthermore, due to the insufficient solubility of the ligands in common solvents and in order to prevent precipitation of the ligands during incubation, an aqueous  $\text{CuCl}_2$  solution and a DMSO solution of the ligands were combined for *in situ* formation of complexes **1–4** (Cu(II):ligand ratio of 1:2.1). An excess of ligand was used to avoid free Cu(II). The nuclease activity of complexes **1–4** in the presence and absence of ascorbate is shown in Fig. 1.

In general, all complexes, and also  $\text{CuCl}_2$ , show better DNA cleavage activity in the presence of ascorbate (in comparison to its absence), which indicates that these Cu(II) species are activated by an external reducing agent and cleave the DNA in an oxidative pathway. Complex **1** is the best DNA cleaving agent as expected from the literature [6–8], for which only DNA fragments were detected under the conditions described above. The nuclease activity decreases in the order **1** > **3** > **4** > **2** (Fig. 1, lanes 5, 7, 9 and 11) in the presence of ascorbate. Complexes **3** and **4** are able to cleave the DNA into its linear form and fragments as well, but to a lesser extent. For **2** mostly supercoiled and nicked DNA were observed. Thus, the conversion of phen into a 5,6-dione (phenD) decreases dramatically the nuclease activity of the corresponding complex.

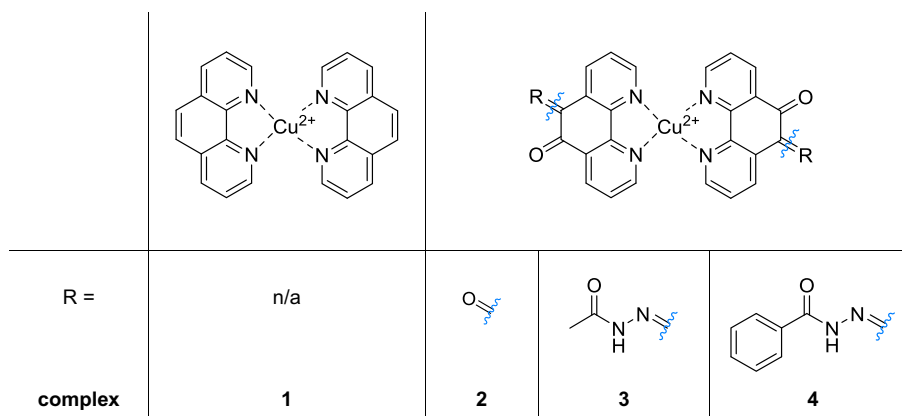


**Chart 1.** Proposed structures of the Cu(II) complexes  $[\text{Cu}(\text{phen})_2]^{2+}$  (**1**),  $[\text{Cu}(\text{phenD})_2]^{2+}$  (**2**),  $[\text{Cu}(\text{phenAH})_2]^{2+}$  (**3**) and  $[\text{Cu}(\text{phenBH})_2]^{2+}$  (**4**) with unsubstituted phen, oxidized phenD and hydrazone-functionalized phenAH and phenBH. Anions and solvent molecules are omitted for clarity. For **3** and **4**, only one of two possible isomers generated by asymmetric substitution at positions 5 and 6 of the phenanthroline moiety is shown.

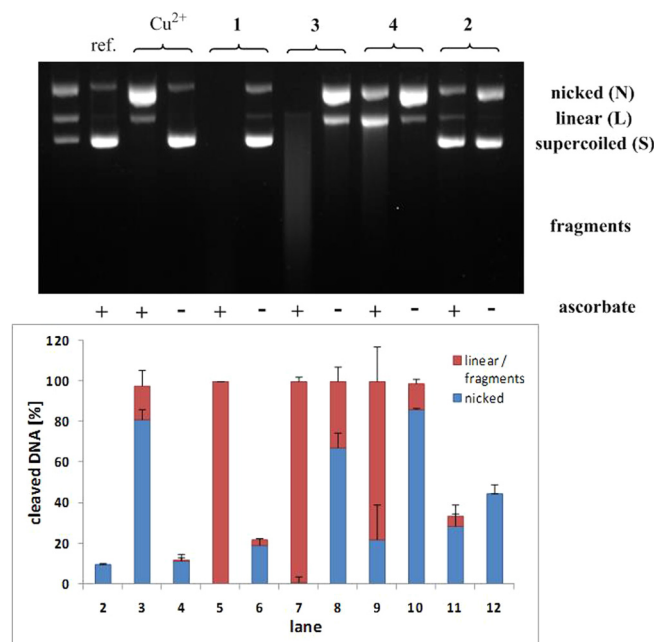


**Fig. 1.** (Top) Cleavage of plasmid DNA pBR322 (0.2  $\mu\text{g}$ ) by  $\text{CuCl}_2$  and complexes **1**, **2**, **3** and **4** in MOPS buffer (50 mM, pH 7.4) after incubation for 2 h at  $37^\circ\text{C}$  in the absence or presence of ascorbate (asc, 1 mM). Lane 1: DNA ladder (S/N/L), lane 2: DNA reference + asc, lane 3:  $\text{CuCl}_2$  (25  $\mu\text{M}$ ) + asc, lane 4:  $\text{CuCl}_2$  (50  $\mu\text{M}$ ), lane 5: **1** (25  $\mu\text{M}$ ) + asc, lane 6: **1** (50  $\mu\text{M}$ ), lane 7: **3** (25  $\mu\text{M}$ ) + asc, lane 8: **3** (50  $\mu\text{M}$ ), lane 9: **4** (25  $\mu\text{M}$ ) + asc, lane 10: **4** (50  $\mu\text{M}$ ), lane 11: **2** (25  $\mu\text{M}$ ) + asc, lane 12: **2** (50  $\mu\text{M}$ ). All samples contained 12.5% DMSO. (Bottom) Visualization of the cleaved DNA in percentage of total DNA. Error bars represent the standard deviation from at least three experiments.

However, an additional functionalization in position 5 to a hydrazone (**3** and **4**) increases the DNA cleavage activity again. As shown below (Sections 3.3 and 3.4), the dione derivatization of phen influences the DNA binding and the redox behavior of the Cu(II)/Cu(I) cycle for generation of ROS in a negative fashion. The hydrazone functionalization reverses this effect with **3** being as active as **1** and **4** achieving an activity close to **1** and **3**.

Surprisingly, in the absence of ascorbate the Cu(II) complexes **2–4** also exhibit DNA cleavage activity. This activity is remarkably high for the hydrazone-functionalized complexes **3** and **4**. Overall, the nuclease activity of complexes decrease in the order **3** > **4** > **2** > **1** (Fig. 1, lanes 8, 10, 12 and 6) in the absence of any external

reducing agent. Thereby, a functionalization (dione or hydrazone) in positions 5 and 6 of the phenanthroline scaffold can have a negative influence in the presence of ascorbate, but has a positive one in the absence of ascorbate. In both cases the complexes with hydrazone-functionalized phenanthrolines (acetyl > benzoyl) show an increased nuclease activity in comparison to the complex with the oxidized form of phenanthroline (phenD).

In order to make sure that the counter ion has no influence on the nuclease activity, we also compared the isolated complexes (nitrate counterions) with *in situ* prepared complexes (chloride counterions) (cf. S12). Indeed, there was no difference in the observed cleavage activity. Also for the isolated complex **3**, for which the suggested composition  $\mathbf{3}(\text{NO}_3)_2 \cdot (\text{H}_2\text{O})_{2.5} \cdot (\text{EtOH})_{0.5}$  does not perfectly fit with the proposed structure (~0.5% deviation), DNA cleavage experiments comparing it to the *in situ* generated complex gave the same results (cf. S12).

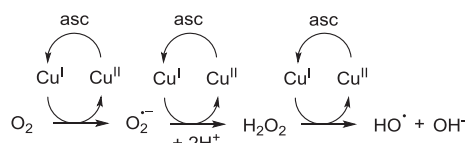
### 3.2.2. Reactive oxygen species (ROS)

To test for an oxidative DNA cleavage mechanism in both the presence and absence of ascorbate, a quench assay for ROS was carried out. In general, Cu(II) metallonucleases with different *N*-donor ligands can cleave the DNA *via* an oxidative cleavage mechanism [28]. Therefore activation with an external reducing agent is generally needed to initiate the generation of ROS through the Cu(II)/Cu(I) redox cycle. A possible pathway for the occurrence of several ROS starting with Cu(II) and ascorbate as a reducing agent is shown in Scheme 1. Such ROS react with DNA by hydrogen abstraction resulting in oxidized ribose and nucleobase moieties and eventually in an irreversible DNA cleavage [12,13].

**3.2.2.1. Presence of a reducing agent.** In order to confirm ROS formation as a cleavage mechanism, quenching experiments were carried out. Representatively, complex **3** (12.5  $\mu\text{M}$ ) was incubated with plasmid DNA pBR322 for 2 h at 37 °C in the presence of ascorbate (1 mM) and ROS scavengers. In Table 1, ROS scavengers are listed with the corresponding reactive species that is quenched [29–32]. In Fig. 2 the nuclease activity of **3** in the absence and presence of the corresponding ROS quenchers is shown.

Compared to the nuclease activity of **3** without any ROS scavenger (lane 3) the activity is decreased in the presence of pyruvate (lane 6) and SOD (lane 7) indicating the presence of hydrogen peroxide ( $\text{H}_2\text{O}_2$ ) and superoxide anion radicals ( $\text{O}_2^{\cdot-}$ ). Thus, an oxidative DNA cleavage pathway by activating Cu(II) with an external reducing agent was proven. The reaction of superoxide anion radicals with SOD (lane 7) leads to hydrogen peroxide [33], which is also a ROS. Not surprisingly, combining SOD with pyruvate (lane 8) results in a more pronounced quenching effect. Additionally, combining all scavengers (lane 9) gives comparable results to the sample with pyruvate and SOD. Consequently, hydroxyl radicals ( $\cdot\text{OH}$ ) and singlet oxygen ( $^1\text{O}_2$ ) can be precluded as ROS in this specific reaction.

It has to be mentioned that all samples contained 12.5% DMSO (corresponds to 1.75 M), a supplement also used in the quenching assay due to its hydroxyl radical scavenging activity, however, usually at lower concentrations (in this case 400 mM). Thus, it cannot



**Scheme 1.** Oxygen reduction by copper redox cycling in the presence of ascorbate and generation of ROS [14,15].

**Table 1**

Scavenger	ROS
DMSO	Hydroxyl radicals ( $\cdot\text{OH}$ ) [29]
$\text{NaN}_3$	Singlet oxygen ( $^1\text{O}_2$ ) [30]
Pyruvate	Hydrogen peroxide ( $\text{H}_2\text{O}_2$ ) [31]
Superoxide dismutase (SOD)	Superoxide anion radicals ( $\text{O}_2^{\cdot-}$ ) [32]

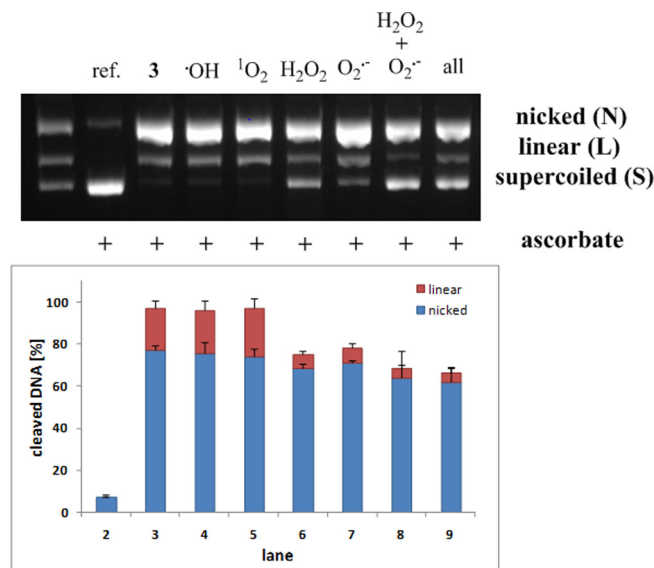


**Fig. 2.** (Top) Cleavage of plasmid DNA pBR322 (0.2  $\mu\text{g}$ ) by complex **3** (12.5  $\mu\text{M}$ ) in MOPS buffer (50 mM, pH 7.4) with ascorbate (1 mM). Incubation for 2 h at 37 °C in the absence and presence of corresponding ROS scavengers. Lane 1: DNA ladder (S/N/L), lane 2: DNA reference, lane 3: **3**, lane 4: **3** + DMSO (400 mM), lane 5: **3** +  $\text{NaN}_3$  (10 mM), lane 6: **3** + pyruvate (2.5 mM), lane 7: **3** + SOD (625 U/mL), lane 8: **3** + pyruvate (2.5 mM) + SOD (625 U/mL), lane 9: **3** + all scavengers. All samples contained 12.5% DMSO. (Bottom) Visualization of the cleaved DNA in percentage of total DNA. Error bars represent the standard deviation from at least three experiments.

be excluded that hydroxyl radicals are formed and are involved in the DNA cleavage.

**3.2.2.2. Absence of a reducing agent.** DNA cleavage activity in the absence of any external activating agent can be caused either by a hydrolytic cleaving pathway or by self-activation through generation of ROS. In order to investigate a potential self-activating property of the artificial metallonucleases, exemplarily, complex **3** was incubated with plasmid DNA pBR322 in the absence of ascorbate for 2 h at 37 °C with the ROS scavengers listed above (Fig. 3).

The quenching experiments for the artificial metallonuclease **3** gave similar results in the presence and absence of ascorbate as an external reducing agent. In both quench assays, hydrogen peroxide ( $\text{H}_2\text{O}_2$ ) and superoxide anion radicals ( $\text{O}_2^{\cdot-}$ ) were the dominant species, even more so in the absence of ascorbate. Thus, the Cu(II) complex **3** initiates an oxidative DNA cleavage pathway also in the absence of a reducing agent. It can be assumed that also the other complexes (**2** and **4**) have such self-activating properties as already indicated from the cleavage activity in the absence of ascorbate (Fig. 1).

The mechanism of self-activating metallonucleases is rarely investigated in the literature. For instance, a hydroxy-salen Cu(II) complex was converted into a Cu(III) species in the presence of oxygen, which caused the generation of superoxide anion radicals as ROS [20]. Cu(III) could also be generated *in situ* by reaction with

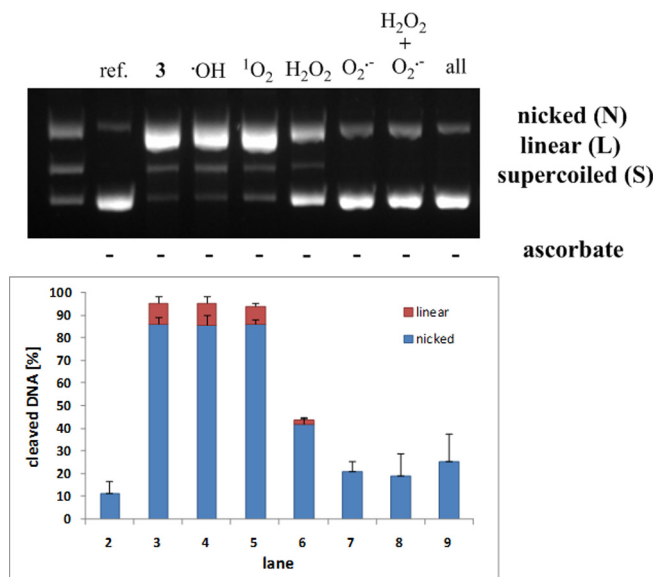


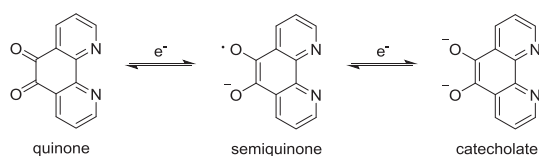
**Fig. 3.** (Top) Cleavage of plasmid DNA pBR322 (0.2 μg) by complex **3** (37.5 μM) in MOPS buffer (50 mM, pH 7.4) **without** ascorbate. Incubation for 2 h at 37 °C in the absence and presence of corresponding ROS scavengers. Lane 1: DNA ladder (S/N/L), lane 2: DNA reference, lane 3: **3**, lane 4: **3** + DMSO (400 mM), lane 5: **3** + NaN<sub>3</sub> (10 mM), lane 6: **3** + pyruvate (2.5 mM), lane 7: **3** + SOD (625 U/mL), lane 8: **3** + pyruvate (2.5 mM) + SOD (625 U/mL), lane 9: **3** + all scavengers. All samples contained 12.5% DMSO. (Bottom) Visualization of the cleaved DNA in percentage of total DNA. Error bars represent the standard deviation from at least three experiments.

a redox non-innocent ligand system like the phenD used here. It has been shown in the literature that phenD is indeed reducible and leads to semiquinone and catecholate species (Scheme 2) [34–36], suggesting such an activation for complex **2**.

In case of phenAH (complex **3**) and phenBH (complex **4**), however, UV/Vis spectra (cf. S11) indicate formation of Cu(I) species in aqueous solution on the basis of broad and intense MLCT bands at ~430 nm and ~550 nm [25]. During incubation with DNA such Cu(I) species can then initiate the generation of ROS as described above and thus lead to damage of this biomolecule (see 3.2.2 and Scheme 1). In the literature, such a self-activation mechanism has been described for Cu(II) complexes with hydrazone or tripyrrolic ligands [17–19]. These oxidizable ligands act as reductants for the generation of Cu(I) species. As suggested by a literature report, oxidation in case of phenAH and phenBH could lead to hydrazoneyl radicals [37].

### 3.2.3. Bis(4-nitrophenyl) phosphate (BNPP) assay

In order to disprove a hydrolytic DNA cleavage mechanism for complexes **2–4**, exemplarily Cu(II) complex **3** (50 and 100 μM) was incubated with bis(4-nitrophenyl) phosphate (BNPP, 50 μM) in MOPS buffer (50 mM, pH 7.4) for 2 h at 37 °C. As a positive control for the cleavage of BNPP, a model for the phosphate backbone of DNA, the enzymatic cleavage by phosphodiesterase I (0.05 U/mL) was used. The hydrolytic cleavage was monitored by UV/Vis spectroscopy by means of the characteristic absorption maximum



**Scheme 2.** Redox equilibrium for *o*-quinone.

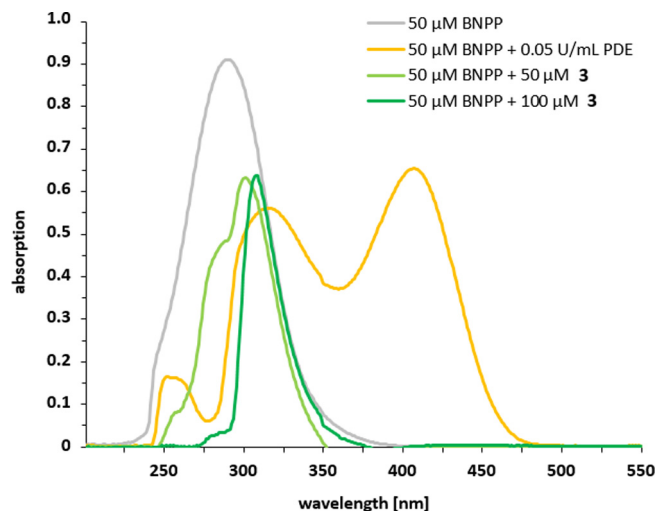


**Fig. 4.** UV/Vis spectra of BNPP (50 μM) after incubation with either **3** (50 μM or 100 μM) or phosphodiesterase I (PDE, 0.05 U/mL). The baseline included all compounds with their respective concentrations except for BNPP. All samples contained 25% DMSO.

of BNPP at 290 nm and of the cleaved product *p*-nitrophenol at 400 nm (Fig. 4).

Due to the fact that after incubation of BNPP with **3** (50 μM or 100 μM) no absorption band in the range of 400 nm was observed, the hydrolytic cleavage mechanism was excluded. Thus, the self-activating character was corroborated, implying an oxidative cleavage mechanism.

**Table 2**

Active Cu(II) species	$E_{1/2}$ [V] of Cu(II)/Cu(I) reduction
<b>1</b>	−0.35
<b>2</b>	−0.92
<b>3</b>	−0.99
<b>4</b>	−0.94

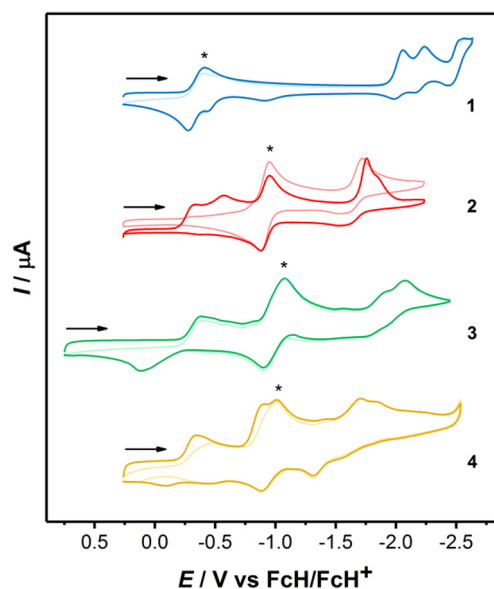


**Fig. 5.** Cyclic voltammograms for the reduction processes of **1–4** in DMF with 0.1 M NBu<sub>4</sub>PF<sub>6</sub> as supporting electrolyte (first cycle: strong line; second cycle: pale line). The supposed Cu(II)/Cu(I) reduction is marked with an asterisk. The ferrocene/ferrocenium redox couple was used as an internal reference. The scan rate was 100 mV/s and the current *I* was normalized.

### 3.3. Cyclic voltammetry

To explain the differing nuclease activity of Cu(II) complexes **1–4**, the redox behavior (by means of cyclic voltammetry) and the extent of DNA interaction can be considered.

With this in mind, the reduction processes of the complexes **1–4** were examined by cyclic voltammetric measurements to obtain the half-wave potential  $E_{1/2}$  of the Cu(II)/Cu(I) redox couple and therefore an insight into the connection between nuclease activity and redox activity of the corresponding Cu(II) complexes. Fig. 5 shows the cyclic voltammograms of **1–4** by using the ferrocene/ferrocenium redox couple as an internal reference. The cyclic voltammograms yield the  $E_{1/2}$  of the reversible Cu(II)/Cu(I) reduction against FcH/FcH<sup>+</sup> (Table 2).

The redox potential for the Cu(II)/Cu(I) reduction decreases in the order  $1 \gg 2 > 4 > 3$ . Furthermore, the Cu(II) complex **1** with unsubstituted phen has by far the least negative redox potential for Cu(II)/Cu(I) reduction, whereas dione- (**2**) and hydrazone-derivatization (**3** and **4**) on the phen scaffold in positions 5 and 6 gives more negative redox potentials, but all in the same range. This can be explained by the initial and favorable reduction of the ligand phenD to a catecholate *via* a semiquinone for **2** and also of phenAH and phenBH to a semiquinone for **3** and **4** (Fig. 5, Scheme 2) [34–36]. Such a reduction is not possible for **1** with

the unsubstituted phen. Thus, the functionalization in 5/6 position shifts the Cu(II)/Cu(I) reduction to more negative potentials.

Bringing the redox activity of the Cu(II)/Cu(I) reduction of **1–4** in accordance with their nuclease activity, **1** should initiate ROS generation to a larger extent in comparison to **2**, **3** and **4** due to its favorable redox potential. Not surprisingly, the Cu(II) complex **1** has the highest nuclease activity. In contrast, the differences in nuclease activity of the functionalized complexes **2**, **3** and **4** can rather be defined by their distinguished mode of binding interaction towards DNA.

### 3.4. CD spectroscopy

Circular dichroism spectroscopy is a commonly used optical technique to investigate the interaction of metal complexes towards DNA due to distinction of different modes of DNA binding such as intercalation and groove binding. In general, CD spectra of CT-DNA exhibit a positive band at 275 nm caused by base-stacking of the nucleobases and a negative band at 245 nm caused by the helicity of the B-form of DNA [38]. A change (increase or decrease) of the positive band corresponds to intercalation of metal complexes and a decrease of the negative band can suggest groove binding interaction [39–41]. The CD spectra of CT-DNA with an increasing amount of the Cu(II) complexes **1–4** are shown in Fig. 6.

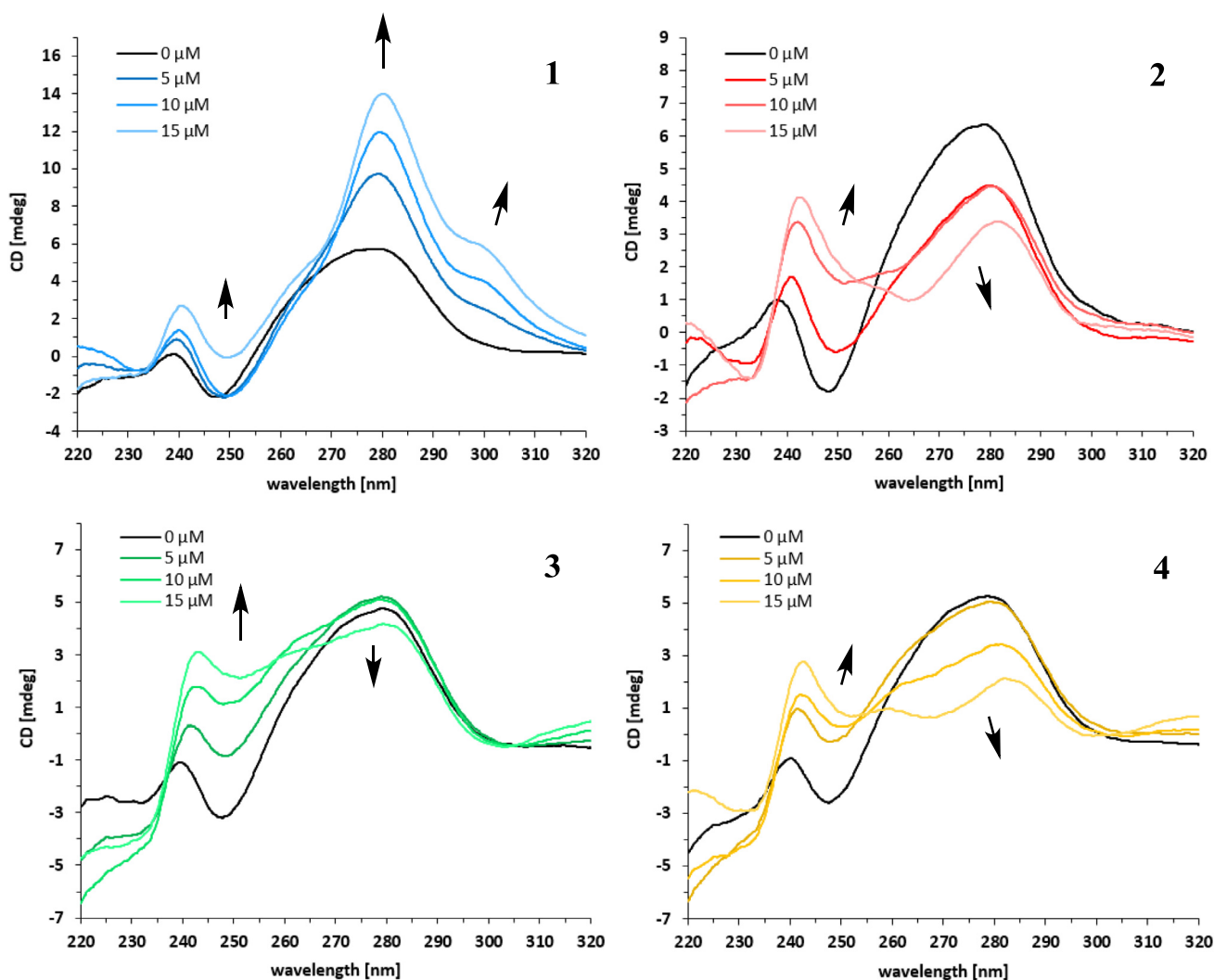


**Fig. 6.** CD spectra of CT-DNA (100 μM) in MOPS buffer (50 mM, pH 7.4) with an increasing amount of Cu(II) complexes **1–4** (0–15 μM) leading to an enhanced alteration of the positive band at 275 nm (base stacking) and the negative band at 245 nm (helicity of B-DNA). All samples contained 10% DMSO.

As expected complex **1** with the unsubstituted phen and thereby planar ligand scaffold caused the strongest change of the positive band at 275 nm due to intercalation in comparison to **2–4**. Whereas complex **1** increases the positive band, complexes **2–4** with functionalized ligands phenD, phenAH and phenBH decrease the positive band, but both indicate intercalation as the DNA binding interaction. Overall, the extent of DNA intercalation decreases in the order **1** >> **4** > **2** > **3** as derived from their CD spectra with CT-DNA. Thus, the nuclease activity of the best DNA cleaving agent **1** in the presence of ascorbate correlates with the DNA binding by means of intercalation and with the redox potential of the Cu(II)/Cu(I) reduction.

In consideration of the negative band at 245 nm due to the helicity of CT-DNA, the strongest change is caused by complex **3**. In general, the order changes to **3** > **2** > **4** > **1** by decreasing the negative band through an assumed groove binding. The complexes **2–4** have nearly the same redox potentials for the Cu(II)/Cu(I) reduction (*cf.* Table 2), but the enhanced nuclease activity of **3** can be explained by an assumed stronger groove binding in comparison to **2** and **4**. Additionally, a hydrazone functionalization with an acetyl moiety (complex **3**) at Cu(II) complex **1** seems to be better for influencing the helicity of CT-DNA than a benzoyl moiety (complex **4**), which again corresponds to the respective DNA cleavage activity.

#### 4. Conclusion

In conclusion, we synthesized the Cu(II) complexes of phen and phenD (**1** and **2**) as well as the Cu(II) complexes of hydrazone-bearing phenAH and phenBH (**3** and **4**), previously not described in the literature. All complexes were characterized *via* elemental analysis, UV/Vis spectroscopy and high resolution ESI mass spectrometry.

DNA cleavage activity was observed in the presence of ascorbate as a reducing agent following the order **1** > **3** > **4** > **2** and in the absence of ascorbate decreasing in the order **3** > **4** > **2** > **1**. Thus, in both cases the hydrazone functionalization in position 5 (acetyl > benzoyl) increases the nuclease activity. In general a derivatization has a positive influence on DNA cleavage in the absence of ascorbate.

The self-activating properties of **2–4** in the absence of any reducing agent were proven by the generation of hydrogen peroxide and superoxide anion radicals in an oxidative DNA cleavage mechanism through an ROS quench assay. Additionally, a hydrolytic DNA cleavage mechanism was excluded by means of a BNPP assay. To the best of our knowledge, we have presented the first Cu(II) metallonucleases on the basis of hydrazone-functionalized phenanthrolines. The self-activating properties of the complexes can be attributed to their redox active ligands and the occurrence of Cu(III) in case of phenD and Cu(I) in case of phenAH and phenBH.

Furthermore, the nuclease activity of the best DNA cleaving agent **1** in the presence of ascorbate as reducing agent correlates with the redox potential of the Cu(II)/Cu(I) reduction ( $E_{1/2} = -0.35$  V) and the DNA binding interaction through intercalation. The differences in nuclease activity of **2–4** despite having nearly the same redox potentials for Cu(II)/Cu(I) reduction ( $E_{1/2} = -0.92$  to  $-0.99$  V) can be explained by additional groove binding, which is strongest for complex **3** with an acetohydrazone functionalization at the phenanthroline.

#### Acknowledgements

We thank Christian Wende for initiating this project, Biprajit Sarkar for useful discussions and the Kulak group for proofreading of this article.

#### Appendix A. Supplementary data

Supplementary data associated with this article can be found, in the online version, at <https://doi.org/10.1016/j.ica.2017.11.015>.

#### References

- [1] P.G. Sammes, G. Yahiolu, *Chem. Soc. Rev.* 23 (1994) 327.
- [2] P. Barbazán, A. Hagenbach, E. Oehlke, U. Abram, R. Carballo, S. Rodríguez-Hermida, E.M. Vázquez-López, *Eur. J. Inorg. Chem.* (2010) 4622.
- [3] M. Carcelli, G. Corazzari, S. Ianelli, G. Pelizzi, C. Solinas, *Inorg. Chim. Acta* 353 (2003) 310.
- [4] M. Carcelli, S. Ianelli, P. Pelagatti, G. Pelizzi, D. Rogolino, C. Solinas, M. Tegoni, *Inorg. Chim. Acta* 358 (2005) 903.
- [5] W.H. Hegazy, M.H. Marzouk, *Chem. Sci. Trans.* 2 (2013) 1482.
- [6] D.S. Sigman, D.R. Graham, V. D'Aurora, A.M. Stern, *J. Biol. Chem.* 254 (1979) 12269.
- [7] D.S. Sigman, C.B. Chen, *Annu. Rev. Biochem.* 59 (1990) 207.
- [8] D.S. Sigman, A. Mazumder, D.M. Perrin, *Chem. Rev.* 93 (1993) 2295.
- [9] G. Verma, A. Marella, M. Shaquiquzzaman, M. Akhtar, M.R. Ali, M.M. Alam, *J. Pharm. Bioallied Sci.* 6 (2014) 69.
- [10] K. Suntharalingam, D.J. Hunt, A.A. Duarte, A.J.P. White, D.J. Mann, R. Vilar, *Chem. Eur. J.* 18 (2012) 15133.
- [11] E.L. Hegg, J.N. Burstyn, *Coord. Chem. Rev.* 173 (1998) 133.
- [12] W. Knapp Pogożelski, T.D. Tullius, *Chem. Rev.* 98 (1998) 1089.
- [13] M.M. Meijler, O. Zelenko, D.S. Sigman, *J. Am. Chem. Soc.* 119 (1997) 1135.
- [14] L. Guilloreau, S. Combalbert, A. Sournia-Saquet, H. Mazarguil, P. Faller, *ChemBioChem* 8 (2007) 1317.
- [15] C. Wende, N. Kulak, *Chem. Commun.* 51 (2015) 12395.
- [16] N.F. König, N. Kulak, Elsevier Reference Module in Chemistry, *Mol. Sci. Chem. Eng.* (2015) 1.
- [17] G. Park, J.T. Tomlinson, M.S. Melvin, M.W. Wright, C.S. Day, R.A. Manderville, *Org. Lett.* 5 (2003) 113.
- [18] M.S. Melvin, J.T. Tomlinson, G.R. Saluta, G.L. Kucera, N. Lindquist, R.A. Manderville, *J. Am. Chem. Soc.* 122 (2000) 6333.
- [19] S. Rodríguez-Hermida, C. Wende, A.B. Lago, R. Carballo, N. Kulak, E.M. Vázquez-López, *Eur. J. Inorg. Chem.* (2013) 5843.
- [20] E. Lamour, S. Routier, J.-L. Bernier, J.-P. Cateau, C. Bailly, H. Vezin, *J. Am. Chem. Soc.* 121 (1999) 1862.
- [21] A. Kellett, M. O'Connor, M. McCann, M. McNamara, P. Lynch, G. Rosair, V. McKee, B. Creaven, M. Walsh, S. McClean, A. Foltyn, D. O'Shea, M. Devereux, *Dalton Trans.* 40 (2011) 1024.
- [22] A. Kellett, M. O'Connor, M. McCann, O. Howe, A. Casey, P. McCarron, K. Kavanagh, M. McNamara, S. Kennedy, D.D. May, P.S. Skell, D. O'Shea, M. Devereux, *Med. Chem. Commun.* 2 (2011) 579.
- [23] W. Guo, B.J. Engelman, T.L. Haywood, N.B. Blok, D.S. Beaudoin, S.O. Obare, *Talanta* 87 (2011) 276.
- [24] Z. Molphy, A. Priscearu, C. Slator, N. Barron, M. McCann, J. Colleran, D. Chandran, N. Gathergood, A. Kellett, *Inorg. Chem.* 53 (2014) 5392.
- [25] O. Das, T.K. Paine, *Dalton Trans.* 41 (2012) 11476.
- [26] P. Hertzberg, P.B. Dervan, *Biochemistry* 23 (1984) 3934.
- [27] J. Nagaj, K. Stokowa-Sołtys, E. Kurowska, T. Frączyk, M. Jeżowska-Bojczuk, W. Bał, *Inorg. Chem.* 52 (2013) 13927.
- [28] C. Wende, C. Lüdtke, N. Kulak, *Eur. J. Inorg. Chem.* (2014) 2597.
- [29] M.K. Eberhardt, R. Colina, *J. Org. Chem.* 53 (1988) 1071.
- [30] K. Li, L.-H. Zhou, J. Zhang, S.-Y. Chen, Z.-W. Zhang, J.-J. Zhang, H.-H. Lin, X.-Q. Yu, *Eur. J. Med. Chem.* 44 (2009) 1768.
- [31] E.A. Mazzi, K.F.A. Soliman, *Neurochem. Res.* 28 (2003) 733.
- [32] J. Hormann, C. Perera, N. Deibel, D. Lentz, B. Sarkar, N. Kulak, *Dalton Trans.* 42 (2013) 4357.
- [33] S.J. Lippard, J.M. Berg, *Principles of Bioinorganic Chemistry*, first ed., University Science Books, Mill Valley, California, 1994.
- [34] L. Michaelis, M.P. Schubert, R.K. Reber, J.A. Kuck, S. Granick, *J. Am. Chem. Soc.* 60 (1938) 1678.
- [35] L. Michaelis, M.P. Schubert, *Chem. Rev.* 22 (1938) 437.
- [36] D.M. Murphy, K. McNamara, P. Richardson, V. Sanchez-Romaguera, R.E.P. Winpenny, L.J. Yellowlees, *Inorg. Chim. Acta* 374 (2011) 435.
- [37] M. Harej, D. Dolenc, *J. Org. Chem.* 72 (2007) 7214.
- [38] V.I. Ivanov, L.E. Minchenkova, A.K. Schyolkina, A.I. Poletayev, *Biopolymers* 12 (1973) 89.
- [39] N. Shahabadi, S. Kashanian, A. Fatahi, *Bioinorg. Chem. Appl.* (2011) 687571.
- [40] P. Uma Maheswari, M. Palaniandavar, *J. Inorg. Biochem.* 98 (2004) 219.
- [41] C. Tong, G. Xiang, Y. Bai, *J. Agric. Food Chem.* 58 (2010) 5257.